Dossier

This paper is a part of the hereunder thematic dossier published in OGST Journal, Vol. 67, No. 2, pp. 187-372 and available online here

Cet article fait partie du dossier thématique ci-dessous publié dans la revue OGST, Vol. 67, n°2, pp. 187-372 et téléchargeable ici

DOSSIER Edited by/Sous la direction de : **F. Roggero**

Monitoring of CO_2 Sequestration and Hydrocarbon Production

Monitoring pour le stockage du CO_2 et la production des hydrocarbures

Oil & Gas Science and Technology – Rev. IFP Energies nouvelles, Vol. 67 (2012), No. 2, pp. 187-372

IFP Energies nouvelles

Oil & Gas Science and Technology – Rev. IFP Energies nouvelles, Vol. 67 (2012), No. 2, pp. 319-328

DOI: 10.2516/ogst/2011162

Impact of Fractures on CO_2 Storage Monitoring: Keys for an Integrated Approach

N. Dubos-Sallée, P.N.J. Rasolofosaon, M. Becquey, C. Putot and B. Zinszner

IFP Energies nouvelles, 1-4 avenue de Bois-Préau, 92852 Rueil-Malmaison Cedex - France
e-mail: noalwenn.sallee@ifpen.fr - patrick.rasolofosaon@ifpen.fr

Résumé — Impact de la présence de fractures pour le monitoring des stockages de CO_2 : éléments pour une approche intégrée — Le monitoring des sites de stockage de CO_2 dans des réservoirs fracturés (champs d'hydrocarbures déplétés ou aquifères salins profonds) nécessite de prendre en compte l'impact de la fracturation et la substitution de fluides sur la réponse sismique. Les données sismiques peuvent fournir des informations sur la souplesse additionnelle due à la présence de fractures et de fluides à travers l'analyse de l'anisotropie sismique azimutale avec un modèle de physique des roches adapté. Nous introduisons un modèle de physique des roches construit en collaboration avec des géologues qui fournit une description réaliste des milieux fracturés. Ce modèle concerne des milieux géologiques fracturés en présence de fluides et qui sont caractérisés par un certain degré de porosité matricielle, la présence de plusieurs familles de fractures connectées ou non avec la porosité matricielle et l'existence d'une anisotropie intrinsèque. L'application directe de ce modèle montre que la valeur de l'anisotropie des ondes *P* mesurée à partir de données sismiques peut être expliquée par plusieurs jeux de paramètres parmi lesquels la densité de fractures, la souplesse du fluide interstitiel ou la porosité. La présence d'une anisotropie inhérente modifie également l'anisotropie des ondes *P* et, par conséquent, l'interprétation de sa valeur en termes de substitution fluide dans un milieu poreux fracturé. En ce qui concerne le monitoring de la substitution fluide, si des données sismiques sont acquises avant et après cette substitution, la modification du niveau d'anisotropie des ondes *P* peut être liée au changement de souplesse du contenu fluide dans le milieu non modifié, présentant le même réseau de fractures et la même porosité. Cette valeur relative d'anisotropie peut être correctement interprétée en termes de substitution fluide, à condition d'avoir des contraintes sur la valeur de quelques paramètres impliqués dans la valeur de l'anisotropie des ondes *P*, comme par exemple la porosité et la souplesse de fractures adimensionnelle. Ainsi, une approche intégrée, multidisciplinaire est nécessaire pour contraindre la valeur de ces paramètres. Par exemple, des informations géologiques provenant des puits et des affleurements peuvent donner une limite supérieure quant à la détermination de la densité de fractures attendue en profondeur. De plus, la mécanique des roches permet de comprendre l'état de fracturation en profondeur pour identifier les fractures prédominantes par rapport à l'interprétation de l'anisotropie sismique en termes de substitution fluide dans un réseau de fractures.

Abstract — Impact of Fractures on CO_2 Storage Monitoring: Keys for an Integrated Approach *— The monitoring of CO_2 storage in fractured reservoirs (depleted hydrocarbon fields or brine aquifers) requires the study of the impact of fracturation and fluid substitution on seismic data. Seismic data can provide information about the additional compliance due to the fractures and the fluids through the analysis of seismic azimuthal anisotropy with an appropriate rock physics model. We introduce a rock physics model built in collaboration with geologists, providing a realistic description of fractured media. This model concerns fractured geological media in the presence of fluids characterized by some degree of matrix porosity, the presence of pore fluids, connected and/or non-connected fractures, the presence of*

several fracture sets, and an inherent seismic anisotropy. The direct application of this rock model shows that the P-wave anisotropy value measured through seismic data can be explained by several sets of different parameters such as the fracture density, the pore fluid compliance or the porosity. The presence of inherent layer-induced anisotropy can also modify the P-wave anisotropy and thus the interpretation of this value in terms of fluid substitution in a fractured porous medium. As far as fluid substitution monitoring is concerned, if seismic data are acquired before and after this substitution, a change in the P-wave anisotropy value can be linked to the modification of the compliance of the fluid content in the same medium exhibiting the same fracture network and the same porosity. This relative value can only be correctly interpreted in terms of fluid substitution provided we have some constraints on a few of the parameters involved in the P-wave anisotropy value such as the porosity, and a rough idea of the level of normalized fracture compliance. Then, a multidisciplinary approach is mandatory to constrain these parameters. For instance, borehole and outcrop geological information can give the upper limit of the fracture density expected at depth in the same formation. Furthermore, rock mechanics helps in understanding the fracturation state at depth to identify the predominant fractures in regard to the interpretation of seismic anisotropy in terms of fluid substitution inside the fracture network.

INTRODUCTION

The monitoring of CO_2 storage in fractured reservoirs (depleted hydrocarbon fields or brine aquifers) requires the study of the impact of fracturation and fluid substitution on seismic data. The presence of sub-seismic fractures (hereafter named fractures for brevity) in several reservoirs is evidenced by much larger permeability derived from production data than expected from core data (matrix permeability) (Bourbiaux *et al*., 2005; Cosentino *et al*., 2001). Several previous studies dealt with the modelling of the influence of fractures on seismic anisotropy (*e.g*., Brown and Lawton, 1993; Fjaer *et al*., 1996; Rasolofosaon, 1998a; Ikelle and Gangi, 2000; Gajewski *et al*., 2003), but we want here to emphasize that a multidisciplinary approach is required in order to finely characterize the impact of fractures on CO_2 storage monitoring. Hence, we will be able to give better representation of the fractured medium in order to significantly reduce prediction uncertainty of flow models used to estimate the long-term fate of stored CO_2 (Bourbiaux *et al*., 2005).

Sophisticated models describing the effect of both fractures and pores on seismic anisotropy have been proposed (Thomsen, 1995; Gurevich, 2003; Cardona, 2002), extending the conventional fracture model of Schoenberg (1980) and the crack model of Hudson (1981). The model used in this study extends the previous models in order to achieve a more realistic description of fractured geological media in the presence of fluids (Dubos-Sallée *et al*., 2008). More precisely, it is characterized by:

- some degree of porosity;
- the presence of multiphasic fluid;
- the presence of connected or non-connected fractures;
- the presence of multiple sets of fractures;
- the presence of inherent seismic anisotropy (*e.g*., due to thin layering, shales, etc.).

From a practical point of view, seismic azimuthal anisotropy is one of the main signatures of the presence of vertical fractures in sedimentary formations (*e.g*., Thomsen, 2002). Furthermore, seismic methods are very useful for extending the description of the fracturation beyond the close vicinity of the wells and for obtaining a description of fractures at a large scale, provided that the presence of the fractures has been confirmed by independent observations such as borehole wall imaging, core samples, well logs, formation tests, etc. In the case where a single family of rotationally invariant and parallel vertical fractures is, if not the only, at least the major cause of seismic anisotropy, the main parameters characterizing fractures are:

- their orientation;
- their consequence on the medium compliance;
- their fluid content;
- their density, and finally;
- the permeability linked to their presence.

These parameters are arranged by increasing interest for reservoir characterization. Unfortunately, the difficulty in estimating these parameters by seismic methods also increases, which clearly illustrates the difficulty of the task.

It is easy to measure the fracture orientation (given, for instance, by the azimuthal variations of the *P*-wave NMO velocity in surface seismics) and the overall compliance of the fractures (*e.g*., Rüger, 1998). The combined use of different types of waves (*P*, *S*, converted waves, etc.) allows one to infer information on both fluid content and fracturation (*e.g*., Thomsen, 2002). In contrast, the evaluation of the remaining parameters (number of fractures per unit length, permeability) is much more difficult and necessitates a complete set of complementary data (wells, production, geology, etc.) and an integrated approach (such as the one we propose). Such data are woefully rare compared with the daunting literature on the topic, as pointed out by Worthington (2006).

In the first part of this paper, we will briefly explain the impact of fractures on seismic anisotropy for non-specialists of geophysics. Secondly, we will describe the petroelastic model developed in collaboration with geologists. In the third

part, we will discuss the predictions of the model and the influence of fracture compliance, porosity and fluid content on seismic anisotropy and the consequences for monitoring purposes. Finally, we will conclude with the importance of an integrated approach to interpret seismic data well.

1 SEISMIC ANISOTROPY DUE TO FRACTURES

The first part of this work is dedicated to a brief explanation on the influence of the presence of fractures on seismic waves that is intended for non-specialists of seismic anisotropy. A complete and very good description of seismic anisotropy for exploration purposes can be found in Helbig (1994).

Fractures and compliant pores are not the only cause of seismic anisotropy. For instance, the presence of horizontal layering in sedimentary formations on a scale much smaller than the seismic wavelength induces an anisotropy called polar anisotropy, or more often Vertical Transverse Isotropy (VTI) (Thomsen, 2002). Besides layer-induced anisotropy, Nur and Simmons (1969) with ultrasonic experiments on rock samples in the laboratory and Gupta (1973a, b) with seismological field data both first experimentally demonstrated the role of oriented cracks/fractures and stresses on seismic anisotropy in geological media. These pioneering works showing the importance of another type of anisotropy, different from polar anisotropy and called azimuthal anisotropy, were significantly extended by Crampin with significant practical applications (*e.g.*, Crampin, 1978, 1981). In the early 1980s everything was ready to demonstrate the potential of vectorial seismology and anisotropic media in the context of seismic exploration (*e.g.*, Thomsen, 1986; Lynn and Thomsen, 1986; Alford, 1986; Willis *et al.,* 1986).

If we consider a medium with a single vertical set of parallel fractures, the manifestation of seismic anisotropy concerns the *P*- and *S*-waves *(Fig. 1)*. The velocity value of the *P*-wave depends on the angle between the ray path and the fracture orientation: the *P*-wave velocity is minimum if the ray path is parallel to the fracture ($V_{\parallel}^{P}$) and maximum if the ray path is normal to the fracture direction ($V_{\perp}^{P}$) *(Fig. 1a)*. Hence, the level of anisotropy for the *P*-wave is given by the well-known parameter ε, roughly equal to the percentage of difference between the fast and slow velocities *(Eq. 1)*:

$$\varepsilon \approx \frac{V_{\parallel}^{P} - V_{\perp}^{P}}{V_{\parallel}^{P}}, \tag{1}$$

A more popular manifestation of seismic anisotropy is the *S*-wave birefringence phenomenon *(Fig. 1b)*. When a *S*-wave coming from an isotropic medium travels through an anisotropic medium, a separation into two waves occurs: in our case, the fastest wave exhibits a polarization parallel to the fracture plane (velocity $V_{\parallel}^{S}$) and the slowest one exhibits a polarization perpendicular to the fracture plane (velocity $V_{\perp}^{S}$). The birefringence phenomenon does not occur in only one case: when the *S*-wave ray path is normal to the fracture plane. The parameter γ is a quantification of the *S*-wave anisotropy *(Eq. 2)*, but contrary to the parameter ε the symbols "perpendicular" and "parallel" concern the orientation of the polarization (and not of the ray path) relative to the fracture plane:

$$\gamma \approx \frac{V_{\parallel}^{S} - V_{\perp}^{S}}{V_{\parallel}^{S}}, \tag{2}$$

As explained previously, fractures are not the only cause of seismic anisotropy and the addition of several cases of anisotropy, such as a layer-induced anisotropy and a fracture-induced anisotropy, implies that the medium can exhibit a

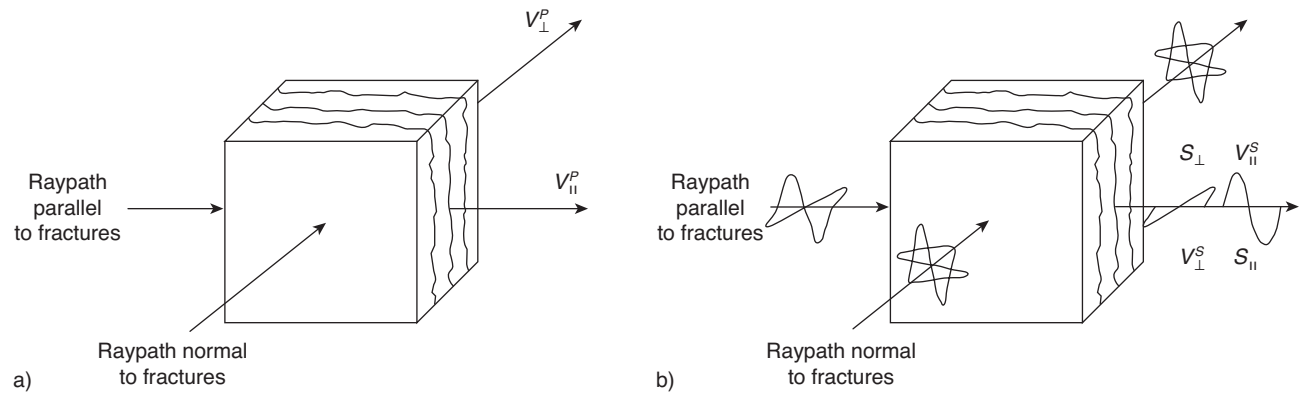

Figure 1

Manifestations of seismic anisotropy due to fractures on *P*- and *S*-waves: a) the fastest *P*-wave velocity is reached for ray path parallel to the fractures ($V_{\parallel}^{P}$), the slowest corresponds to a ray path normal to the fractures ($V_{\perp}^{P}$); b) a *S*-wave coming from an isotropic medium is split into two *S*-waves ($S_{\parallel}$ and $S_{\perp}$) in an anisotropic medium: the fastest *S*-wave exhibits a polarization parallel to the fracture ($V_{\parallel}^{S}$), the slowest one exhibits a polarization perpendicular to the fracture plane ($V_{\perp}^{S}$).

more complicated anisotropy symmetry type. In such cases, the development of general equations concerning the seismic wave behavior is tricky (Helbig, 1994). In the specific case of moderate anisotropy strength, simple analytical expressions for kinematic and dynamic quantities of interest for seismic processing can be obtained, specially for *P*-waves (Mensch and Rasolofosaon, 1997).

In this study, we do not use this well-documented description of the effect of seismic anisotropy on kinematics or on the determination of seismic reflectivity coefficients. As explained in detail in the next section, the aim of this work is to provide a model described by parameters which allow one to give a more realistic (geological!) description of fractured geological media in the presence of fluids.

2 ROCK PHYSICS MODEL INVOLVING FRACTURES

The petroelastic model we propose *(Sect. 2.4)* issues from several discussions with geologists. Geologists want geophysicists to introduce fracturation into a rock physics model which can correspond to what they observe in the field. Hence, geophysicists have to achieve a more realistic description of a fractured geological medium than the idealized description of the fracturation by specific geometrical shape such as penny-shape and with a single orientation. So, after some discussions with geologists, we propose this model, which concerns fractured geological media in the presence of fluids characterized by some degree of matrix porosity, the presence of pore fluids, connected and/or non-connected fractures, the presence of several fracture sets, and an inherent seismic anisotropy.

2.1 The Biot-Gassmann Model

Linear isotropic poroelastic theory was introduced by Biot (1941). The relations between the macroscopic parameters of Biot's theory and the microscopic parameters of the porous medium and of the saturating fluid can be found in Gassmann (1951). These elements are briefly given here. For further details, please refer to the original articles.

The undrained bulk and shear moduli, respectively K_{und} and μ_{und}, of a rock are linked to the corresponding drained bulk and shear moduli, respectively K_{dry} and μ_{dry}, by the relations:

$$K_{und} = K_{dry} + b^2 M \;;\; \mu_{und} = \mu_{dry} \tag{3}$$

The b coefficient is known as the Biot effective stress coefficient and M is the pressure to be exerted on saturating fluid to increase the fluid content by a unit value in a non-deforming frame (Bourbié *et al.*, 1987). The Gassmann theory (Gassmann, 1951) gives the link between the macroscopic parameters b and M and the microscopic parameters describing the medium. The undrained bulk and shear moduli, respectively K_{und} and μ_{und}, of a rock are linked to the porosity (Φ), the bulk modulus of the saturating fluid (K_{fl}), the density of the saturating fluid (ρ_{fl}), the bulk modulus of the solid intact matrix, or equivalently the grain constituent (K_{grain}), the density of the solid intact matrix or grain constituent (ρ_{grain}), the bulk modulus of the drained rock (K_{dry}) and the shear modulus of the drained rock (μ_{dry}). The Gassmann theory gives the following relations:

$$b = 1 - \frac{K_{dry}}{K_{grain}} \quad ; \quad \frac{1}{M} = \frac{\Phi}{K_{fl}} + \frac{(b-\Phi)}{K_{grain}} \tag{4}$$

2.2 Anisotropic Poroelastic Theory

The anisotropic poroelastic theory is described by Brown and Korringa (1975) and Cheng (1997). The anisotropic relations corresponding to the previous are:

$$K^{und}_{ijkl} = K^{dr}_{ijkl} + b_{ij} b_{kl} M, \tag{5}$$

with:

$$b_{ij} = \delta_{ij} - K^{dr}_{ijkl} S^{grain}_{klmm}, \tag{6}$$

and:

$$\frac{1}{M} = K^{dr}_{ijmn} S^{grain}_{mnll} \left(S^{dr}_{ijkk} - S^{grain}_{ijkk} \right) + \Phi \left(C^{fluid} - S^{grain}_{iikk} \right) \tag{7}$$

In these relations, summation convention on repeated indices is assumed. $K^{(.)}_{ijkl}$ and $S^{(.)}_{ijkl}$ respectively designate the components of the stiffness tensor and of the compliance tensor of the considered material ((.) corresponds to "*und*" for undrained medium, to "*dr*" for drained medium, to "*grain*" for grain constituent or to "*fl*" for saturating fluid), and δ_{ij} the unit symmetric tensor of rank 2, or Kronecker tensor. Cheng (1997) called the symmetric tensor b_{ij} the Biot effective stress coefficient tensor. The parameter C^{fluid} is the fluid compressibility.

In the isotropic case, four macroscopic parameters are sufficient to describe a porous medium: K_{dry}, μ_{dry}, b and M. Whereas in the general case, an anisotropic medium is described by the 21 elastic components of the tensor K^{dr}_{ijkl}. If this medium also exhibits a matrix porosity, seven other parameters are necessary: the six components of the symmetric tensor b_{ij} and the scalar coefficient M.

2.3 Description of a Non-Porous Fractured Medium: Schoenberg's Theory

We consider a homogeneous isotropic medium with a single fracture, considered as a plane of mechanical discontinuity exhibiting a negligible width in regard to the seismic wavelength. This fracture separates two identical media *(Fig. 2)*. The parameters describing the fracture model are:

– the solid matrix elastic parameters (λ and μ), and;

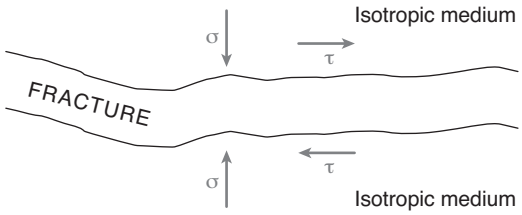

Figure 2

Fracture separating two identical isotropic media. σ and τ correspond, respectively, to the compressive and the shear stresses.

– the fracture stiffness parameters K_N (normal) and K_T (tangential) linked to the compressive (σ) and shear (τ) stresses by the relations:

$$\sigma = K_N \Delta u \quad ; \quad \tau = K_T \Delta v \tag{8}$$

where Δu and Δv correspond, respectively, to the normal and tangential displacement discontinuities induced by the seismic wave. The normal and tangential fracture stiffnesses, respectively designated by K_N and K_T, characterize the quality of the mechanical coupling between the isotropic media separated by the fracture. More precisely, in the case of perfectly cemented fractures, no displacement discontinuity is induced by the wave ($\Delta u = \Delta v = 0$ in the previous relations). As a consequence, K_N and K_T must be infinite to allow the wave-induced stresses σ and τ to be finite values. The opposite limit case is when K_N and K_T vanish ($K_N = K_T = 0$). In this case the wave-induced stresses σ and τ also vanish. This simply corresponds to completely open fractures which totally reflect the incident wave.

Schoenberg and Douma (1988) consider isotropic media affected by the presence of n fractures per length unit in the direction normal to the fracture planes. Each of these fractures exhibit the same behaviour as the fracture described above. These fractures are parallel to each other and randomly distributed in the media. The elastic components of the compliance tensor of the fractured medium can be written as:

$$S_{ijkl} = S^m_{ijkl} + \delta S^{frac}_{ijkl} \tag{9}$$

where S^m_{ijkl} is the matrix (or intact rock) compliance and δS^{frac}_{ijkl} is the additional compliance due to the presence of fractures.

We can distinguish two fracture properties, a "normal fracture density" (ε_N) and a "tangential fracture density" (ε_T), directly linked to the dimensionless normal and tangential fracture compliances E_N and E_T through the following relations:

$$\varepsilon_N = \frac{E_N}{1+E_N} \quad ; \quad \varepsilon_T = \frac{E_T}{1+E_T} \tag{10}$$

The parameters E_N and E_T are linked to the normal and tangential fracture stiffnesses K_N and K_T, by the relations:

$$E_N = \frac{n(\lambda + 2\mu)}{K_N} \quad ; \quad E_T = \frac{n\mu}{K_T} \tag{11}$$

with n the number of fractures per unit length.

2.4 How Anisotropic Poroelastic Theory and Non-Porous Fractured Media Theory are Combined

We use the model of Dubos-Sallée *et al*. (2008). The main elements of the theoretical work are explained here. The proposed petroelastic model can consider connected and non-connected fractures. The connected fractures correspond to the fractures connected to the porous network and that can be involved in the wave-induced fluid displacement. Hence, the non-connected fractures correspond to fractures that are not involved in this macroscopic fluid displacement.

So, the drained compliance tensor S^{dr}_{ijkl} of the medium is corrected by the presence of the connected fracturation and the compliance tensor S^{grain}_{ijkl} of the intact matrix is corrected by the presence of the non-connected fracturation. The following corrections are applied using the Schoenberg formalism and replaced Equation (9):

$$corr\_S^{dr}_{ijkl} = S^{dr}_{ijkl} + \delta S^{conn.frac.}_{ijkl} \tag{12}$$

and

$$corr\_S^{grain}_{ijkl} = S^{grain}_{ijkl} + \delta S^{non-conn.frac.}_{ijkl} \tag{13}$$

Furthermore, if several sets of fractures are considered, the compliance correction due to each fracture set is added to the compliance of the material considered (medium or grain), the interaction between the fracture families being neglected.

The last step of the model is to apply the anisotropic poroelastic theory of the previous section to the new porous medium characterized by the new drained compliance tensor and the new grain compliance tensor.

3 IMPACT FOR SEISMIC MONITORING

3.1 Direct Application

In this part, we present typical predictions of the model for a sandstone exhibiting an inherent Vertical Transverse Isotropy and a fracture-induced anisotropy due to a family of vertical parallel fractures. We define the azimuth-dependent *P*-wave anisotropy as the difference between the horizontal velocity $V^P_{\text{horizontal}}(\text{az})$ for the considered azimuth and the vertical velocity V^P_{vertical} normalized by the vertical velocity. Figure 3 shows the value of the *P*-wave anisotropy as a function of the azimuth of observation for different pore fluids (gas or water) and different porosities (5% or 15%).

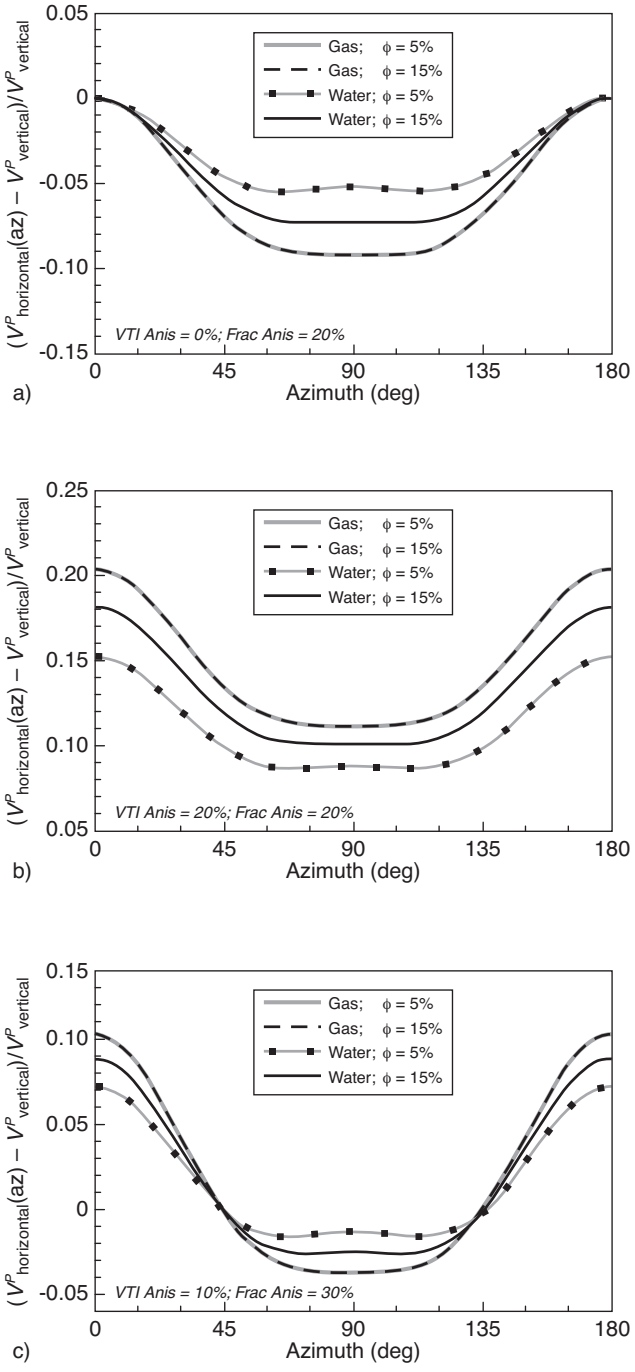

Figure 3

Predictions of the model for a sandstone exhibiting an inherent Vertical Transverse Isotropy and a fracture-induced anisotropy due to a family of vertical parallel fractures (fracture azimuth: 0°). *P*-wave anisotropy as a function of the azimuth of observation for different pore fluids (gas or water) and different porosities (5% or 15%). Three combinations of VTI and fracture-induced anisotropies are given:

a) VTI anisotropy 0% and fracture-induced anisotropy 20%;

b) VTI and fracture-induced anisotropy 20%;

c) VTI anisotropy 10% and fracture-induced anisotropy 30%.

The first case *(Fig. 3a)* concerns a fracture-induced anisotropy of 20% (the fracture azimuth is 0°) with no other cause of anisotropy. In the direction parallel to the fracture, there is no *P*-wave anisotropy, as expected. Actually, for this azimuth, the vertical *P*-wave velocity and the horizontal *P*-wave velocity are identical, leading to this null value. For the other azimuths, the horizontal *P*-wave velocity is affected by the presence of fractures and becomes smaller than the vertical *P*-wave velocity. That is the reason why the *P*-wave anisotropy value is negative with our definition. The *P*-wave anisotropy value is more and more negative with azimuth until reaching its maximum absolute value in the direction perpendicular to the fracture. We can notice slight variations between 0° and 90°; for instance, for the curve corresponding to a water content and a matrix porosity of 5% *(Fig. 3a)*. In fact, contrary to the *P*-wave NMO velocity, the mathematical expression of the *qP*-wave velocity in a weakly anisotropic medium of arbitrary symmetry type is not elliptical and exhibits local maxima and minima, leading to the observed slight variations (Mensch and Rasolofosaon, 1997; Rasolofosaon, 2000).

The second case *(Fig. 3b)* concerns the same medium as before with an additional inherent layer-induced anisotropy of 20%. The maximum of *P*-wave anisotropy is reached for the fracture azimuth, as expected: it is actually a well-known method to obtain this orientation. When gas is the pore fluid, the value of the *P*-wave anisotropy for the fracture direction corresponds to the VTI level chosen: 20%. In this direction, parallel to the fracture, there is no anisotropy due to fractures and the fluid inside the fracture is too compliant to stiffen the fracture. That is the reason why the prediction gives 20%. For water as a fluid content, it is no longer the case: the presence of a less compliant fluid makes the fracture stiffer and so decreases the anisotropy. The inherent VTI anisotropy exhibits a symmetry axis perpendicular to the symmetry axis of the fracture-induced anisotropy. Hence, as long as the azimuth increases until a direction normal to the fracture, the VTI anisotropy is progressively thwarted by the presence of the fracture-induced anisotropy. For the same reason, from 90° to 180° the influence of fracture-induced anisotropy on the *P*-wave anisotropy is more and more weak, leading to a value corresponding to the inherent VTI anisotropy chosen for azimuth 180°. We can also add for this second case *(Fig. 3b)* that the influence of the matrix porosity is weak for highly compliant fluid, such as gas, but it is no longer the case for water, for instance, for which different porosities lead to different *P*-wave anisotropy profiles.

Figure 3c concerns another combination of layer-induced and fracture-induced anisotropies: the VTI anisotropy is weaker than in the previous case and the fracture anisotropy is stronger. In return, fluid contents and porosities are similar to those used to build Figure 3b. For the azimuth corresponding to fracture orientation, we can make the same comments given for the previous case: for a compliant fluid, the *P*-wave

anisotropy level is the inherent VTI anisotropy of the medium. Furthermore, for this azimuth, the more compliant the fluid, the higher the *P*-wave anisotropy. For greater azimuths, the fracture-induced anisotropy progressively makes up for the inherent VTI anisotropy. Beyond an azimuth close to 45°, the influence of the presence of a huge amount of fractures is very strong. Hence, the additional compliance introduced by fractures into the medium leads to a situation for which vertical *P*-wave velocity becomes greater than the horizontal one. As a consequence, the *P*-wave anisotropy is then negative *(Fig. 3c)*. This phenomenon is enhanced by the compliance of the fluid content: if we consider absolute values, the more compliant and at a second order the more porous it is, the more anisotropic it is.

3.2 A Scalar Quantity Can Impact the Seismic Anisotropy

We have briefly seen in the previous section that a scalar parameter, the porosity, can influence a tensorial property, the seismic anisotropy. Hence, this part is dedicated to a little close-up on this non-intuitive impact. Thomsen (1995) considers this influence on elastic anisotropy due to aligned fractures. If fractures are connected to the matrix porosity, the fluid content can leave the fracture to go into the pore space. Whereas the fluid content tends to stiffen the fracture, if the porosity is great enough to allow the "leak" into the pore space, the compliance of the fractures increases and thus seismic anisotropy also. Figure 4 concerns the *P*-wave anisotropy value in the vertical plane perpendicular to the fracture azimuth, as a function of matrix porosity for a sandstone exhibiting three normalized fracture compliances, five different pore fluids and two inherent VTI anisotropies (0% and 20%). The fracture compliance is the fracture density multiplied by the compliance of a single fracture. The normalized fracture compliance is the fracture compliance relative to the matrix compliance *(Eq. 11)*. Hence, Figure 4a corresponds to the context described by Thomsen (1995): a unique cause of anisotropy (fractures) and a homogeneous porous matrix. These results of our model confirm that the porosity has an impact on seismic anisotropy in the vertical plane normal to the fracture set, even if the porosity is a scalar quantity. The matrix porosity impacts our rock model through the Gassmann formulation: the undrained stiffness tensor is a function of the drained stiffness tensor and the matrix porosity where the matrix porosity weighted in a way the drained stiffness tensor. So, if the drained stiffness or compliance tensor is affected by the presence of connected fractures, the matrix porosity will emphasize this influence. As far as seismic anisotropy is concerned, gaseous CO_2 and supercritical CO_2 have the same impact in our model. For this

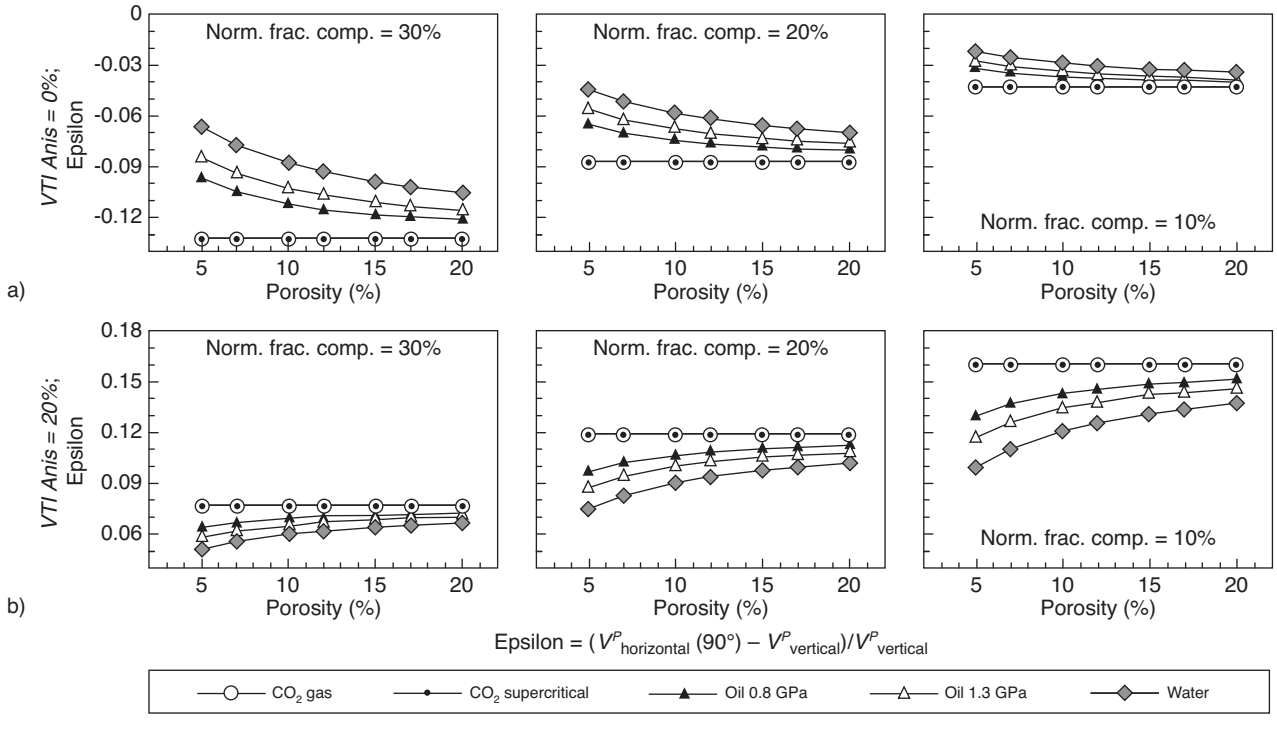

Figure 4

P-wave anisotropy in the vertical plane normal to the fracture set (Epsilon) as a function of matrix porosity of a sandstone exhibiting three normalized fracture compliances (10%, 20% and 30%), five different pore fluids and two inherent VTI anisotropies: a) 0%, b) 20%.

first case *(Fig. 4a)*, we can conclude again that the *P*-wave anisotropy value increases with the normalized fracture compliance, the compliance of the fluid content and the matrix porosity.

Figure 4b corresponds to a medium exhibiting an inherent layer-induced anisotropy of 20% and three different levels of fracture-induced anisotropy described through three different values of normalized fracture compliance (10%, 20% and 30%). Because of the influence of the VTI anisotropy, the maximum of the *P*-wave anisotropy, in the vertical plane perpendicular to the fracture set, is reached for the smallest normalized fracture compliance. For this level of normalized fracture compliance (10%), the horizontal *P*-wave velocity is in fact weakly impacted. Hence, the *P*-wave anisotropy value remains close to the VTI anisotropy as far as compliant fluid content is concerned (see *Fig. 4b* Epsilon = 0.16). For more compliant fluid contents, the *P*-wave anisotropy is impacted by the variation of the vertical *P*-wave velocity. The presence of a less compliant fluid, such as water, inside the porous medium makes the medium stiffer and thus increases the vertical *P*-wave velocity, leading to a decrease in the *P*-wave anisotropy. This stiffening phenomenon is enhanced in a medium exhibiting a low porosity.

For the highest normalized fracture compliance (30%), the impact of the layer-induced anisotropy is considerably thwarted *(Fig. 4b)*. Actually, in this case, the horizontal *P*-wave velocity is greatly influenced by the presence of fractures and becomes very close to the vertical *P*-wave velocity whatever the fluid content and the porosity.

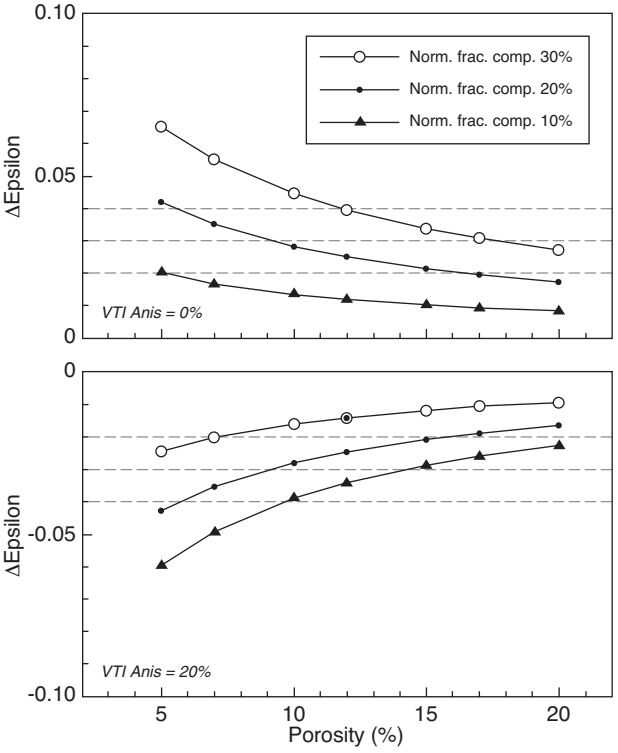

Figure 5

Variation of *P*-wave anisotropy value due to the substitution of *in situ* water by CO_2 in a supercritical state as a function of matrix porosity, taking into account two inherent layer-induced anisotropies (0% and 20%) and three levels of normalized fracture compliances (10%, 20% and 30%).

3.3 Implication for Fluid Substitution Monitoring

The main consequence of the results discussed in the two previous sub-sections concerns the fact that the absolute value determined for the *P*-wave anisotropy from seismic methods is not straightforward to interpret since different parameters are involved in anisotropy.

In the case of CO_2 geological storage, the *in situ* fluid, which can be brine, oil or a mixture of oil and brine or water, is generally substituted by CO_2 in a supercritical state. So, if seismic data are acquired before and after this substitution, a change in the *P*-wave anisotropy (ΔEpsilon in *Fig. 5*) can be measured, which is clearly linked to the modification of the compliance of the fluid content in the same medium exhibiting the same fracture network and the same porosity. This relative value can only be correctly interpreted in terms of fluid substitution provided we have some constraints on a few of the parameters involved in the *P*-wave anisotropy value such as the porosity, and a rough idea of the level of normalized fracture compliance.

Figure 5 corresponds to the change in *P*-wave anisotropy due to a substitution of *in situ* water by CO_2 in a supercritical state as a function of matrix porosity, taking into account two inherent layer-induced anisotropies (0% and 20%) and three levels of normalized fracture compliances (10%, 20% and 30%). For instance, in a VTI medium, a change in the *P*-wave anisotropy value of –0.04 can correspond to a fluid substitution in a sandstone exhibiting a matrix porosity of 6% and a normalized fracture compliance of 20%, or in a sandstone exhibiting a matrix porosity of 10% and a normalized fracture compliance of 10%. If we consider a medium without inherent VTI anisotropy a ΔEpsilon of 0.04 can correspond to a fluid substitution in a sandstone exhibiting a matrix porosity of 6% and a normalized fracture compliance of 20%, or in a sandstone exhibiting a matrix porosity of 12% and a normalized fracture compliance of 30%.

Hence, if we want to monitor the fluid substitution in a fracture network of a CO_2 storage site, we have to precisely define the matrix porosity and the fracture compliance and thus the fracture density. It is the reason why an integrated approach is necessary. Seismic data alone can give the orientation of the fracture and the overall compliance, but cannot discriminate the parts of the different parameters in this compliance we have described here. Outcrop observations, if

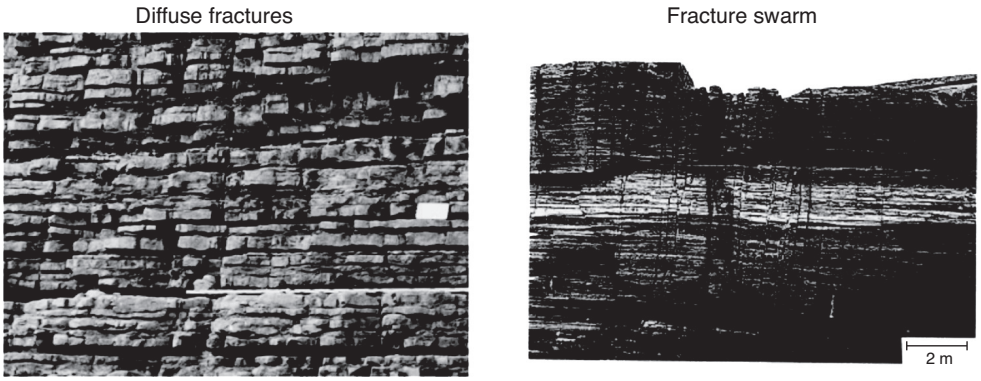

Figure 6

Two fracture network types found in sedimentary formations with weak tectonic structures: diffuse fracturation (left) and fracture swarms (right) (after Auzias, 1995).

they are available, and representative of what happens at depth, can give us information about the type of fracture. Generally, two fracture network types can be found in sedimentary formations with weak tectonic structures. The first type concerns diffuse fractures, extremely common in well-bedded formations. These fractures are generally perpendicular to the beds and exhibit no relative displacement between two blocks separated by the fracture *(Fig. 6)*. The distance between two fractures is linked to the bed thickness. Some fractures are due to stress relaxation, so the fracture density observed has to be considered as an upper limit of what we can expect at depth. The second type concerns fracture swarms, which may affect tabular zones *(Fig. 6)*. They cut several beds with no displacement and are characterized by the presence over a relatively short width of a great number of vertical fractures with very low spacing.

As the rock physics model used considers a constant density of fracturation in the investigated volume, the confirmation of the presence at depth of such fracture swarms, thanks, for instance, to deviated wells, has to be taken into account through the compartmentalization of the reservoir as far as the study of *P*-wave anisotropy is concerned.

The information obtained via borehole imaging interpretation can also give an idea of the fracture density in specific areas and this data has to be used keeping in mind the possibility that it is not necessarily representative of the large-scale network. We also have to wonder about the state of stress at depth that determines which sets of fractures can be considered as the predominant ones in regard to the interpretation of seismic anisotropy and fluid substitution inside the fracture network. The matrix porosity also has to be specified as finely as possible on several core samples to limit the uncertainty that would lead to a greater uncertainty on fracture compliance and on the monitoring of the fluid substitution in geological storage of CO_2.

CONCLUSION

We have described the petroelastic model developed in collaboration with geologists which concerns fractured geological media in the presence of fluids, characterized by some degree of matrix porosity, the presence of pore fluids, connected and/or non-connected fractures, the presence of several fracture sets, and an inherent seismic anisotropy. We have also shown the *P*-wave anisotropy predicted by our model in different configurations, taking into account inherent VTI anisotropy or not, a single vertical fracture network and different fluid contents. These configurations are representative of subsurface media which can be involved in CO_2 geological storage. As explained in Section 1, the measurement of the *P*-wave anisotropy is an appropriate and relevant method to identify the fracture network orientation and the fluid substitution in a fracture set provided time-lapse seismic data are available. Nevertheless, the results shown in this study illustrate how different parameters can influence the *P*-wave anisotropy such as normalized fracture compliance, the compliance of the fluid content and the matrix porosity, even if the porosity is a scalar parameter. Hence, the absolute value measured for *P*-wave anisotropy from seismic data acquisition is not explained by a unique set of these parameters.

The monitoring of the fluid substitution inside a fracture network benefits greatly from 4D seismics since it is a good way to avoid the difficult interpretation of the absolute value of *P*-wave anisotropy. Furthermore, we are also convinced by the benefit of a multidisciplinary approach to correctly interpret the part of the seismic anisotropy due to the fractures and thus to monitor geological storage of CO_2 better.

ACKNOWLEDGMENTS

This work was supported by the French National Research Agency (ANR) under the program "*Captage et Stockage du CO_2*", as part of the project "EMSAPCO$_2$" (ANR-07-PCO2-001, 2008 to 2010). We thank the anonymous referees for their careful reviews.

REFERENCES

Alford R.M. (1986) Shear data in the presence of azimuthal anisotropy, *56th Annual International SEG Meeting*, Houston, USA, Expanded abstracts, pp. 476-479.

Auzias V. (1995) Contribution à la caractérisation tectonique des réservoirs fracturés, *PhD Thesis*, University of Montpellier II, France.

Biot M.A. (1941) General theory of three-dimensional consolidation, *J. Appl. Phys.* **12**, 155-164.

Bourbiaux B., Basquet R., Daniel J.M., Hu L.Y., Jenni S., Lange A., Rasolofosaon P.N.J. (2005) Fractured Reservoir Modelling: A Review of the Challenges and some recent solutions, *First Break* **23**, 9, 33-40.

Bourbié T., Coussy O., Zinszner B. (1987) *Acoustics of Porous media*, Ed. Technip, Paris.

Brown R.J.S., Korringa J. (1975) On the dependence of the elastic properties of a porous rock on the compressibility of the pore fluid, *Geophysics* **40**, 4, 608-616.

Brown R.J.S., Lawton D.C. (eds) (1993) *Proceedings of the 5th International Workshop on Seismic Anisotropy*, Banff, Alberta, Canada, May 17-22, 1992, Can. *J. Explor. Geophys.* **29**, 1.

Cardona R. (2002) Two theories for fluid substitution in porous rocks with aligned cracks, *72nd SEG Annual Meeting and International Exhibition*, Salt Lake City, Utah, USA, October 6-11, Expanded abstracts, Paper ANI, Vol. 3.5.

Cheng A.H.D. (1997) Material Coefficients of Anisotropic Poroelasticity, *Int. J. Rock Mech. Min. Sci.* **34**, 2, 199-205.

Cosentino L., Coury Y., Daniel J.M., Manceau E., Ravenne C., Van Lingen P., Cole J., Sengul M. (2001) Integrated Study of a Fractured Middle East Reservoir with Stratiform Super-K Intervals - Part 2: Upscaling and Dual Media Simulation, *Paper SPE* 68184, presented at the *SPE Middle East Oil Show*, Bahrain, 17-20 March.

Crampin S. (1978) Seismic wave propagation through a cracked solid: Polarization as a possible dilatancy diagnostic, *Geophys. J. Roy. Astron. Soc.* **53**, 467-496.

Crampin S. (1981) A review of wave motion in anisotropic and cracked elastic media, *Wave Motion* **3**, 343-391.

Dubos-Sallée N., Becquey M., Putot C., Rasolofosaon P.N.J., Zinszner B. (2008) Impact of fractures on CO_2 storage monitoring - An integrated approach, *First EAGE CO_2 Geological Storage Workshop*, Budapest.

Fjaer E., Holt R.M., Rathore J.S. (eds) (1996) Seismic Anisotropy, *Proceedings of the 6th International Workshop on Seismic Anisotropy*, Trondheim, Norway, July 03-08, 1994, Society of Exploration Geophysicists, Tulsa.

Gassmann F. (1951) Über die Elastizitätporösen Medien, *Vierteljahrsschrift der Naturforschenden Gesellschaft in Zurich* **96**, 1-23.

Gajewski D., Vanelle C., Psencık I. (2003) *Proceedings of the 10th International Workshop on Seismic Anisotropy*, Tutzing, Germany, April 14-19, 2002, *J. Appl. Geophys.* **54**, 3-4.

Gupta I.N. (1973a) Dilatancy and premonitory variations of P, S travel times, *Bull. Seismol. Soc. Am.* **63**, 3, 1157-1161.

Gupta I.N. (1973b) Premonitory variations in *S*-wave velocity anisotropy before earthquakes in Nevada, *Science* **182**, 4117, 1129-1132.

Gurevich B. (2003) Elastic properties of saturated porous rocks with aligned fractures, *J. Appl. Geophys.* **54**, 3-4, 203-218.

Helbig K. (1994) *Foundations of Anisotropy for Exploration Seismics*, Pergamon, New-York.

Hudson J.A. (1981) Wave speeds and attenuation of elastic waves in material containing cracks, *Geophys. J. Roy. Astron. Soc.* **64**, 133-150.

Ikelle L., Gangi T. (eds) (2000) Anisotropy 2000: Fractures, Converted Waves and Case Studies, *Proceedings of the 9th International Workshop on Seismic Anisotropy*, Houston, USA, March 26-31, Society of Exploration Geophysicists, Tulsa.

Lynn H., Thomsen L. (1986) Shear-wave exploration along the principal axes, *56th Annual International SEG Meeting*, Houston, USA, Expanded abstracts, pp. 473-476.

Mensch T., Rasolofosaon P.N.J. (1997) Elastic wave velocities in anisotropic media of arbitrary symmetry - Generalization of Thomsen's parameters ε, δ and γ, *Geophys. J. Int.* **128**, 43-64.

Nur A., Simmons G. (1969) Stress-induced velocity anisotropy: An experimental study, *J. Geophys. Res.* **74**, 27, 6667-6674.

Rasolofosaon P.N.J. (ed.) (1998a) *Proceedings of the 8th International Workshop on Seismic Anisotropy*, Boussens, France, April 20-24, 1998, *Oil Gas Sci. Technol.* **53**, 5.

Rasolofosaon P.N.J. (2000) From transverse isotropy to arbitrary anisotropy for *qP*-waves in weakly anisotropic media, in *Anisotropy 2000: Fractures, converted waves and case studies*, Ikelle L., Gangi T. (eds), *Transactions of the 9th International Workshop on Seismic Anisotropy*, Society of Exploration Geophysicists, Tulsa.

Rüger A. (1998) Variation of *P*-wave reflectivity with offset and azimuth in anisotropic media, *Geophysics* **63**, 3, 935-947.

Schoenberg M. (1980) Elastic behavior across linear slip interfaces, *J. Acoust. Soc. Am.* **68**, 5, 1516-1521.

Schoenberg M., Douma J. (1988) Elastic wave propagation in media with parallel fractures and aligned cracks, *Geophys. Prospect.* **36**, 6, 571-590.

Thomsen L. (1986) Reflection seismology in azimuthally anisotropic media, *56th Annual International SEG Meeting*, Houston, USA, Expanded abstracts, pp. 468-470.

Thomsen L. (1995) Elastic anisotropy due to aligned cracks in porous rock, *Geophys. Prospect.* **43**, 6, 805-829.

Thomsen L. (2002) Understanding seismic anisotropy in exploration and exploitation, *SEG/EAGE Distinguished Instruction Short Course*, No. 5, SEG Tulsa.

Willis H., Rethford G., Bielanski E. (1986) Azimuthal anisotropy: Occurrence and effect on shear wave data quality, *56th Annual International SEG Meeting*, Houston, USA, Expanded abstracts, pp. 476-479.

Worthington M.H. (2006) The visibility of fluid-filled macro-fractures, *12th Int. Workshop on Seismic Anisotropy*, Beijing, China, October 22-27.

Final manuscript received in July 2011
Published online in April 2012